

Dear Dr. Jordi Vila-Guerau de Arellano,

We would like to first thank you for your very kind and constructive comments. We would like to reply your comments point by point in sections.

## 1. Introduction

Thank you very much for your very positive comments on the introduction, and your suggestion for additional points and references to make the introduction more complete. We have added the following highlighted sentence in the first paragraph of the introduction to address your point about the two origins of chemical segregation:

Turbulence mixes initially-segregated reactive species in the boundary layer, and allows chemical reactions to occur. However, for fast chemical reactions with the chemical timescale shorter than the turbulent timescale, turbulent motions mix the reactants so slowly that they remain segregated rather than reacting. This segregation can be a result of the inefficient mixing due to the state of turbulence and its driver, such as thermal stability, canopy-atmosphere interaction and cloud processes, and/or a result of the heterogeneity of surface emissions (Vilà-Guerau de Arellano, 2003).

The two references you have suggested are also added in the introduction (see highlighted text in the introduction paragraphs):

Many of these LES studies focus on the convective boundary layer, in which the imbalance between updraft and downdraft transport produces a large segregation of the reactants (Wyngaard and Brost, 1984; Chatfield and A. Brost, 1987). Such LES studies were often performed with idealised cases with a bottom-up tracer emitted from the surface and top-down tracer entrained from the free troposphere with a simple second-order chemistry scheme. For instance, Schumann (1989) pointed out that the segregation between the two tracers depends on the Damköhler number ( $Da$ ), the concentration ratio of the two species and the specified initial conditions, pinning the use of  $Da$  as an indicator to estimate whether turbulent motions are significantly affecting chemical reactions in the flow. Vinuesa and Vilà-Guerau de Arellano (2005) introduced the concept of an effective chemical reaction rate ( $k_{eff}$ ) to quantify the actual boundary layer-averaged reaction rate that accounts for the effect of the chemical segregation. They also reported a drop of  $k_{eff}$  up to 20% from the imposed chemical reaction rate  $k$  when  $Da \sim 1$ , while  $k_{eff} \sim k$  when  $Da \sim 0.1$ . Recently, the effect of segregation due to inefficient turbulent mixing on chemical reaction has been considered as the cause of the miscalculation of large-scale models in a number of scenarios. One of the most discussed issues is the under-prediction of the concentration of hydroxyl radical (OH) in global models. A number of studies employed LES models over forestal areas with sophisticated chemical mechanisms involving biogenic VOCs to simulate the resultant segregation between isoprene and OH (e. g. Patton et al. (2001); Brosse et al. (2017); Dlugi et al. (2019)). However, the magnitude of the segregation coefficient  $I_S$  shown in these studies is in general less than 20%, which is too small to explain the observed discrepancy, where  $I_S \sim 50\%$  is necessary (Butler et al., 2008).

The aim of the present work is to investigate the effect of inefficient turbulent mixing on chemical reactions in an urban-like boundary layer with strong and heterogeneously-distributed surface emissions, and to account for the errors induced by neglecting the resultant subgrid chemical segregation in relatively coarse regional models. While previous studies focused on agricultural and rural conditions where the emission fluxes are relatively low ( $\sim O(0.01)$  ppb m s<sup>-1</sup>), our simulations address cases of strong emission fluxes in typical urban values ( $\sim O(0.1-1.0)$  ppb m s<sup>-1</sup>). In two rare related studies in urban air condition, Baker et al. (2004) reported from their LES model of an urban street canyon significant deviations of the concentrations of the NO-NO<sub>2</sub>-O<sub>3</sub> triad from the equilibrated values to the photostationary state depending on the turbulent structure in the canyon; while Auger and Legras (2007) obtained high values of instantaneous segregation under certain emission configurations in urban areas with a chemical system of 44 species. On top of their conclusions, our study aims to explain why this strong segregation occurs under urban conditions and on which parameters the errors induced by neglecting the segregation in large-scale models depend. To achieve this aim, we perform DNS simulations with homogeneous emissions with an idealised second-order A-B-C chemistry scheme (A+B→C) with emission fluxes extended to urban values, in addition to a set of simulations with heterogeneous emissions. With varied reaction rates, the idealised second-order A-B-C chemistry scheme can generally represent any second-order chemical reactions commonly seen in an urban environment.

## 2. Model description

It is a pleasure to hear that you find the direct numerical simulation technique a plus to the research of the topic.

(a) The Kolmogorov timescale is around 10 s for all the simulations. We adopt the definition of the corresponding Kolmogorov Damköhler number in Vilà-Guerau de Arellano et al. (2004). The definition of the corresponding Kolmogorov Damköhler number is added in the manuscript in Section 2.3 after the description of the Damköhler number:

To quantify the chemical-turbulence interaction at the molecular diffusion spatiotemporal scale, the Kolmogorov Damköhler numbers are also calculated in some of simulations. The definition of Kolmogorov Damköhler number is adopted from Vilà-Guerau de Arellano et al. (2004), i.e.:

$$Da_{k,A} = \frac{t_k}{t_{chem,A}}$$

for Tracer A, and similarly for Tracer B ( $Da_{k,B}$ ) by replacing the denominator with  $t_{chem,B}$ . The Kolmogorov timescale  $t_k$  is around 10 s for all the simulations (Garcia and Mellado, 2014).

Since the dynamical settings of the DNS simulations in the paper are the same (except for the longer simulation time for the heterogeneous runs), the Kolmogorov Damköhler numbers of the runs are equal to the Damköhler numbers provided in Table 2 in the original draft divided by the ratio between the convective and Kolmogorov timescale (around 79.8). The resultant Kolmogorov Damköhler numbers are given in Table 1 of this document. For comparison, we have replotted Figure 8 of the original draft to include an additional  $x$ -axis with the limiting Kolmogorov Damköhler number ( $Da_{k,lim}$ ) (see Figure 1 of this document). The errors induced by neglecting the subgrid chemical segregation become significant when  $Da_{k,lim}$  reaches the order of around  $10^{-1}$ . We will replace Figure 8 of the original manuscript with Figure 1 of this document, and to add the following highlighted text addressing this issue in Section 3.13:

Since the chemical transformation of the reactant that is relatively less abundant than the other reactant is influenced more by turbulent mixing (Vilà-Guerau de Arellano et al., 2004),  $Da_{B,f}$  is now a better indicator for the role of turbulent mixing on chemical reactions than  $Da_{A,f}$ . Summarising the simulations with homogeneous emissions, one can observe from Figure 8 (black circles) that the deviation of  $k_{eff}$  from the imposed rate  $k$ , or the error from the complete-mixing model, increases with the increased Damköhler number of the limiting reactant ( $Da_{lim}$ ), where  $Da_{lim} = Da_{A,f}$  when the reaction is Tracer A-limiting and  $Da_{lim} = Da_{B,f}$  when the reaction is Tracer B-limiting. This transition occurs when  $Da_{lim}$  reaches the order of 10. Similar concept can also be applied to the corresponding Kolmogorov Damköhler number, where the limiting Kolmogorov Damköhler number ( $Da_{k,lim}$ ) is introduced (refer to the upper  $x$ -axis of Figure 8). The errors induced by neglecting the subgrid chemical segregation become significant when  $Da_{k,lim}$  reaches the order of around  $10^{-1}$ .

(b) Section 2.2.1: We have performed another set of simulations with the NO-NO<sub>2</sub>-O<sub>3</sub> chemical system with increasing NO emission fluxes, which include the backward reaction of NO<sub>2</sub> → NO + O<sub>3</sub>. The details of the simulation settings can be found in Section 3.5 of the doctoral thesis of CWYL (available at [https://pure.mpg.de/pubman/faces/ViewItemOverviewPage.jsp?itemId=item\\_3069134](https://pure.mpg.de/pubman/faces/ViewItemOverviewPage.jsp?itemId=item_3069134)). As a comparison we have plotted the resultant errors ( $E$ ) in that set of simulations over the limiting Damköhler number ( $Da_{lim}$ ) in Figure 1 in this document (green circles). One can see that the resultant errors are smaller in all cases with NO-NO<sub>2</sub>-O<sub>3</sub> chemical system as compared to those in the A-B-C chemical system. However, as  $Da_{lim}$  reaches  $\sim O(10)$ , the increase in  $E$  is not as large as

that with the A-B-C chemical system. The error increases to around 15%, instead of  $> 80\%$  with the A-B-C chemical system. Also, this error does not increase with  $Da_{lim}$  once the  $Da_{lim}$  reached  $O(10)$ , contrary to the increasing trend observed in the A-B-C chemical system. This phenomenon agrees with what was reported in Jonker et al. (2004). Unfortunately we cannot apply the analytical solution proposed in Jonker et al. (2004) to calculate the concentrations with a backward reaction, as in some of our simulations with large emission fluxes, the concentrations of Tracer A and B do not reach equilibrium at the end of the simulations (but the variances of the concentrations do). Therefore including a backward reaction may require reruns of the simulations. We therefore add the following highlighted text to discuss this above-mentioned summary points from the doctoral thesis of CWYL and add a suggestion to include a backward reaction in future simulation studies in the Discussion:

Unlike other studies (e. g. Ouwersloot et al. (2011); Dlugi et al. (2019); Kim et al. (2016); Li et al. (2016, 2017)) in which 30 multiple-reaction chemical systems are employed, our work mostly focuses on an idealised second-order chemical reaction of two non-specific reactive species. This approach allows us to interpret our work for any second-order chemical reactions. For a chemical species involved in a multiple-reaction chemical system, like  $O_3$ , one can still calculate the net impact of chemical segregation by considering the errors of all reactions in which the species is involved. However, it is also important to notice that the net impact of chemical segregation on such a species would in general be reduced with the increasing complexity of the chemical system, because cycling reactions tend to lengthen the chemical timescale and reduce the corresponding Damköhler number, and hence reduce the chemical segregation. For example, with emission fluxes of  $NO_X$  comparable to our sflux and ssflux cases, the segregation coefficient between isoprene and OH is only  $-0.05$  and  $-0.17$  in the high- and very high- $NO_X$  cases of Kim et al. (2016) respectively. Li (2019) also performed simulations similar to this study with the  $NO-NO_2-O_3$  triad, and found less significant errors than with the A-B-C chemical system. Also, this error does not increase with  $Da_{lim}$  when  $Da_{lim}$  reached the order of 10, contrary to the increasing trend observed in the A-B-C chemical system. Therefore we expect the magnitude of chemical segregation to be smaller than the values reported in this study when a multiple-reaction chemical system is included. Future studies can also consider implementing a backward reaction in addition to the idealised second-order chemical reaction to approximate the effect of a multiple-reaction chemical system.

### 3. Results

(a) Figure 2: The time-averaged cross-section of the production term for the last 30 minutes of the simulation is shown in Figure 2 in this document. It will be included in the next revision of our manuscript.

(b) Section 3.1.2: The maxima near the top of the surface layer are found at an altitude of around 60 m. While this height corresponds to around 8.73 vertical levels in our DNS model, it corresponds to 2.34 vertical levels in the LES model used in Vinuesa and Vilà-Guerau de Arellano (2005). As the segregation coefficient is relatively sensitive to the change in altitude in this region, the lower vertical resolution would underestimate the slope of the vertical profile of the segregation coefficient in that layer. Although the LES model includes subgrid parametrisation, it is anticipated to show similar effect as in the coarse-grid model analysis (compare the vertical profiles of  $k_{eff}/k$  between the DNS model and the coarse-grid models in Figure 9).

(c) Figure 3: Attached please see the plots of the exchange coefficients of Tracer A, B and C for the different cases addressed in Figure 3. For all Tracers, the magnitudes of their exchange coefficients are still more significant in the mixed layer. Their magnitudes at the surface and in the encroachment zone are still relatively small. At the surface, the no-slip condition was implemented in the DNS code, so that the turbulent fluxes are always equal to zero, resulting a zero exchange coefficient. In the encroachment zone, the large turbulent fluxes are counterbalanced by the large concentration gradient, so that the exchange coefficients are again relatively small. Note that the relatively “noisy” profiles of the exchange coefficients of Tracer B and C in the mixed layer are due to the very small concentration gradients of the two tracers in the mixed layer. The level of “noisiness” of these profiles may hinder the meaningfulness of including these profiles in the discussion. However, the profiles of Tracer A show better “signal-to-noise” ratios. Also note that as

the emission fluxes of Tracer A increases (mflux - ssflux), the corresponding exchange coefficients are almost the same between the slow- and fast-chemistry cases.

(d) Section 3.2 (line 29): Please refer to point 2(b) in this reply.

(e) Figure 9: As the segregation can be related to the standard deviations of the concentrations of the tracers (Vinuesa and Vilà-Guerau de Arellano, 2005), we have attached the vertical profiles of the concentration variances of Tracer A, B and C in Figure 4 in this document. One can see that for all tracers in all cases, the concentration variances in the encroachment zone are always larger than those near the surface. This difference is even larger for Tracer B and C. Therefore one may anticipate a large segregation and hence a lower  $k_{eff}/k$  in the encroachment zone than near the surface.

#### 4. Discussion

The points you have suggested are all very insightful and worth considering.

(a) Section 5.1 : As the chemical segregation is affected by many initial and boundary conditions and also the combination of these conditions, it is very difficult to formulate a parametrisation that can be applied to every scenario. Under these circumstances, look-up tables that describe the segregation or  $k_{eff}/k$  under specific conditions may serve as an alternative to parametrisations so that modellers can choose the right tables that best describe the scenarios they want to simulate. The following highlighted text are added in the corresponding paragraph in Section 5.1:

One important aim of the study of chemistry-turbulence interaction is to provide a correction to the error in large-scale model induced by neglecting subgrid chemical segregation. While our work suggests a correction of  $k_{eff}$  with dependencies on  $Da_{lim}$  and  $dx$ , other work suggest that such correction should also include other variables such as updraft/downdraft fluxes (Petersen and Holtslag, 1999), variance of the reacting species, entrainment/emission fluxes (Petersen and Holtslag, 1999; Vinuesa and Vilà-Guerau de Arellano, 2003), turbulent fluxes (Dlugi et al., 2014), variance of the emission (Galmarini et al., 1997), magnitude and direction of mean horizontal wind (Ouwersloot et al., 2011) and distance from the sources (Karamchandani et al., 2000). There have been attempts to implement a parametrisation of subgrid chemistry-turbulence interaction to large-scale models. For example, Molemaker and Vilà-Guerau de Arellano (1998) suggested the use of lookup tables to indicate how chemical reaction rates should be corrected under different physical or chemical scenarios. Lenschow et al. (2016) developed a one-dimension second-order closure model to account for the vertical turbulent mixing of chemical species ready to be incorporated into large-scale models. Given that the effect of subgrid chemical segregation is non-negligible under urban conditions, modellers should consider applying similar parametrisations in areas with intense emission and large source heterogeneity.

(b) P. 17 Line 1: Previous work on natural canopies will definitely be useful to be connected to urban canopies. First of all, we can use the results on natural canopies to estimate/extrapolate the effect on urban canopies. Second, as the vegetation are always mixed within the urban canopies in many cities, it would be also useful to combine the features of natural and urban canopies in future simulations on the topic. The following highlighted text are added in Section 5.2:

An important source of surface forcings in an urban boundary layer is undoubtedly from the urban structures (buildings and streets in the urban canopy). The structure of turbulent flow can be significantly altered in the street canyons due to the exchange of heat and momentum with the urban structures (e. g. Oke (1997)). Therefore, our DNS simulations are more suitable in addressing the vertical mixing caused by the turbulent motions in the mixed layer relatively far away from the surface features that may induce other additional forcings. But in the mixed layer, the urban canopy still potentially affects the chemistry and dynamics in the boundary layer by means of surface roughness and emission heterogeneity. While in this work we have addressed the effect of emission heterogeneity, the effect of surface roughness and other configurations of emission patterns (e. g. Auger and Legras (2007)) can be further studied in the future. Previous work on natural canopies can also be combined to further studies with urban canopies as the vegetation are mixed within the urban canopies in many cities.

We truly hope that our reply and revisions to the manuscript can answer most of your concerns and questions on the current version of the manuscript.

#### References:

1. Jonker, H. J., Vilà-Guerau de Arellano, J., & Duynkerke, P. G. (2004). Characteristic length scales of reactive species in a convective boundary layer. *Journal of the atmospheric sciences*, *61*(1), 41-56.
2. Vilà-Guerau de Arellano, J., Dosio, A., Vinuesa, J. F., Holtslag, A. A., & Galmarini, S. (2004). The dispersion of chemically reactive species in the atmospheric boundary layer. *Meteorology and Atmospheric Physics*, *87*(1-3), 23-38.
3. Vinuesa, J. F., & Vilà-Guerau de Arellano, J. (2005). Introducing effective reaction rates to account for the inefficient mixing of the convective boundary layer. *Atmospheric Environment*, *39*(3), 445-461.

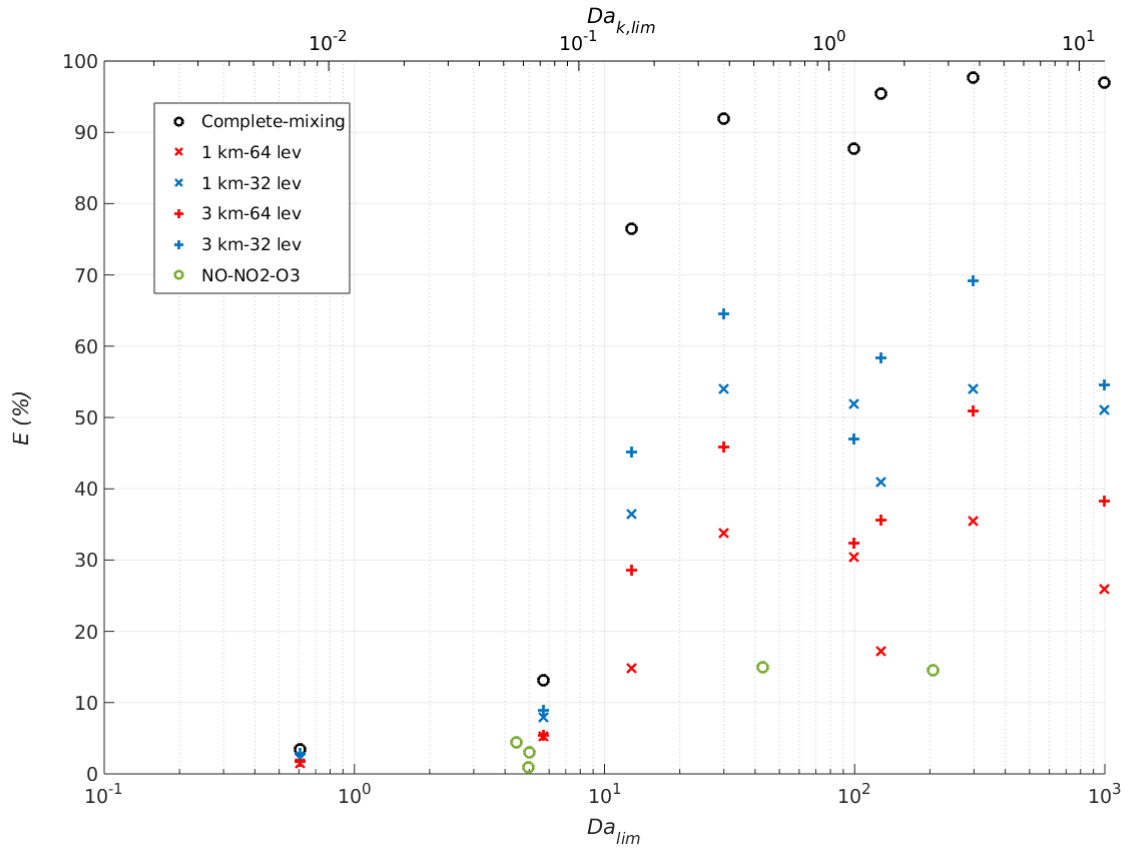


Figure 1: Replot of Figure 8 in the manuscript. An additional  $x$ -axis with the limiting Kolmogorov Damköhler number ( $Da_{k,lim}$ ) (top  $x$ -axis) and the results of the DNS simulations with NO-NO<sub>2</sub>-O<sub>3</sub> chemical system (circles in green) are added. The latter will not be shown in the next revision of the manuscript.

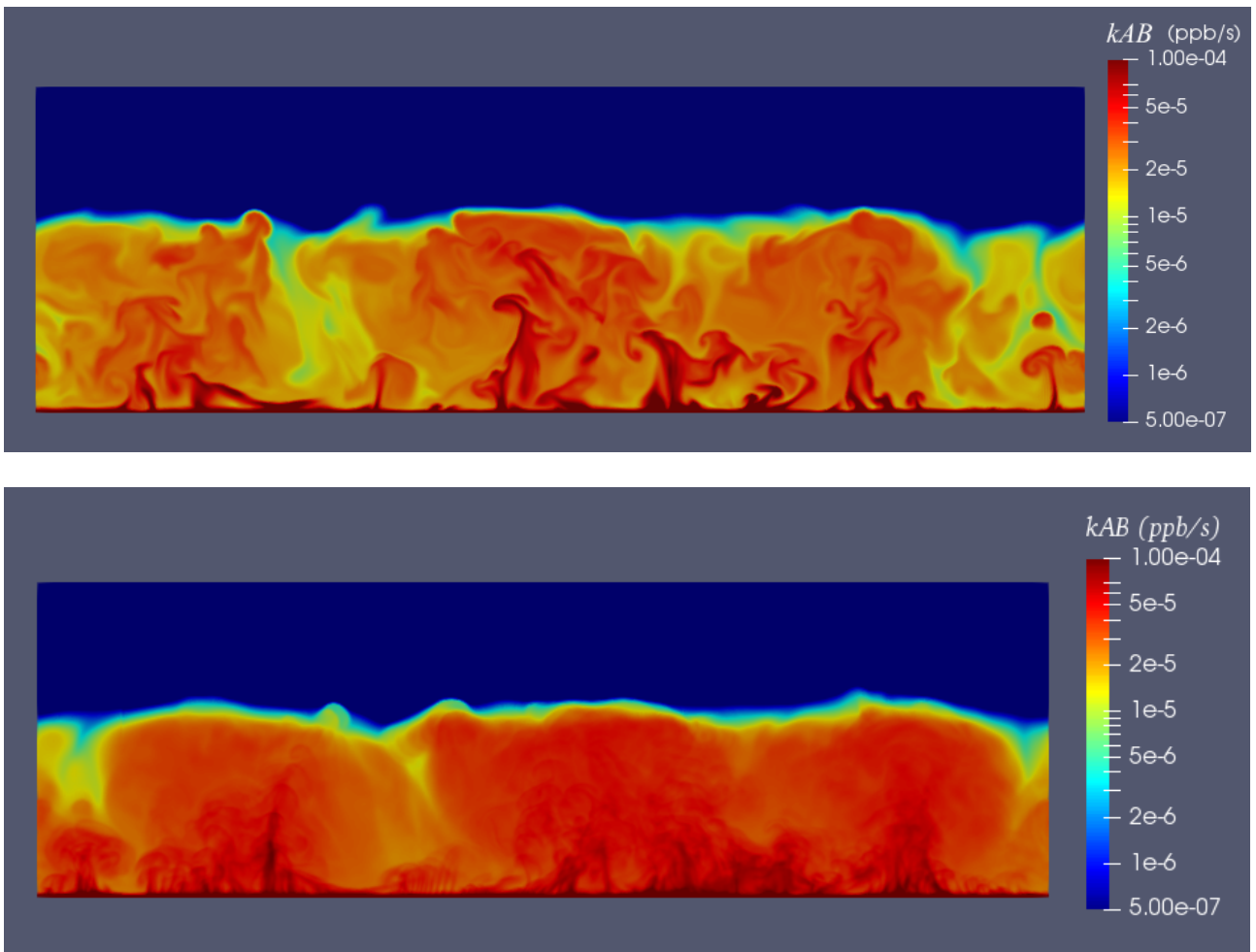


Figure 2: The top panel of Figure 2 in the manuscript (*top panel*) and the color map of the same simulation with a time-averaged field of the production field over the last 30 minutes of the simulation (*bottom panel*).



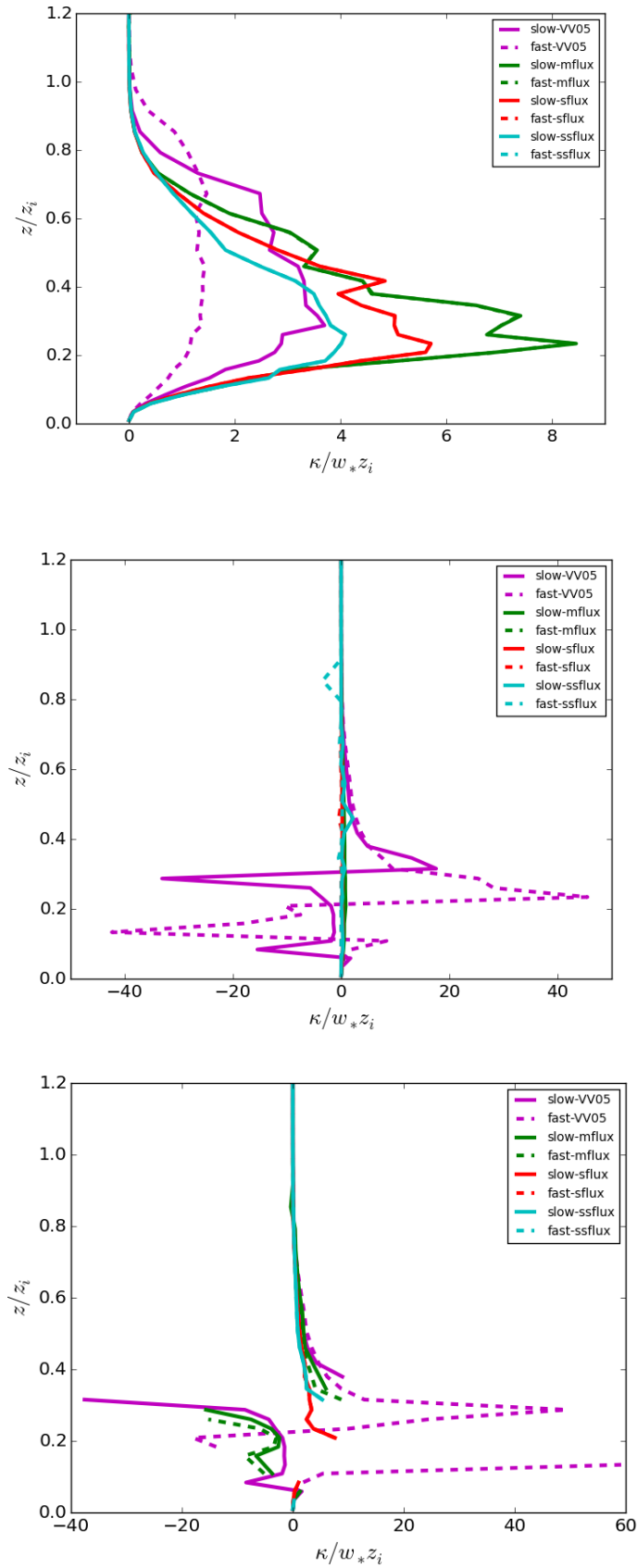


Figure 3: The vertical profiles of the horizontally-averaged exchange coefficients ( $\kappa$ ) of Tracer A (*top panel*), B (*middle panel*) and C (*bottom panel*) normalised by the product of the boundary layer height  $z_i$  and the convective velocity  $w_*$ . Here the same simulation cases are shown as in Figure 3 of the manuscript. The data here are averaged every 8 vertical levels to lessen the effect of the noise.



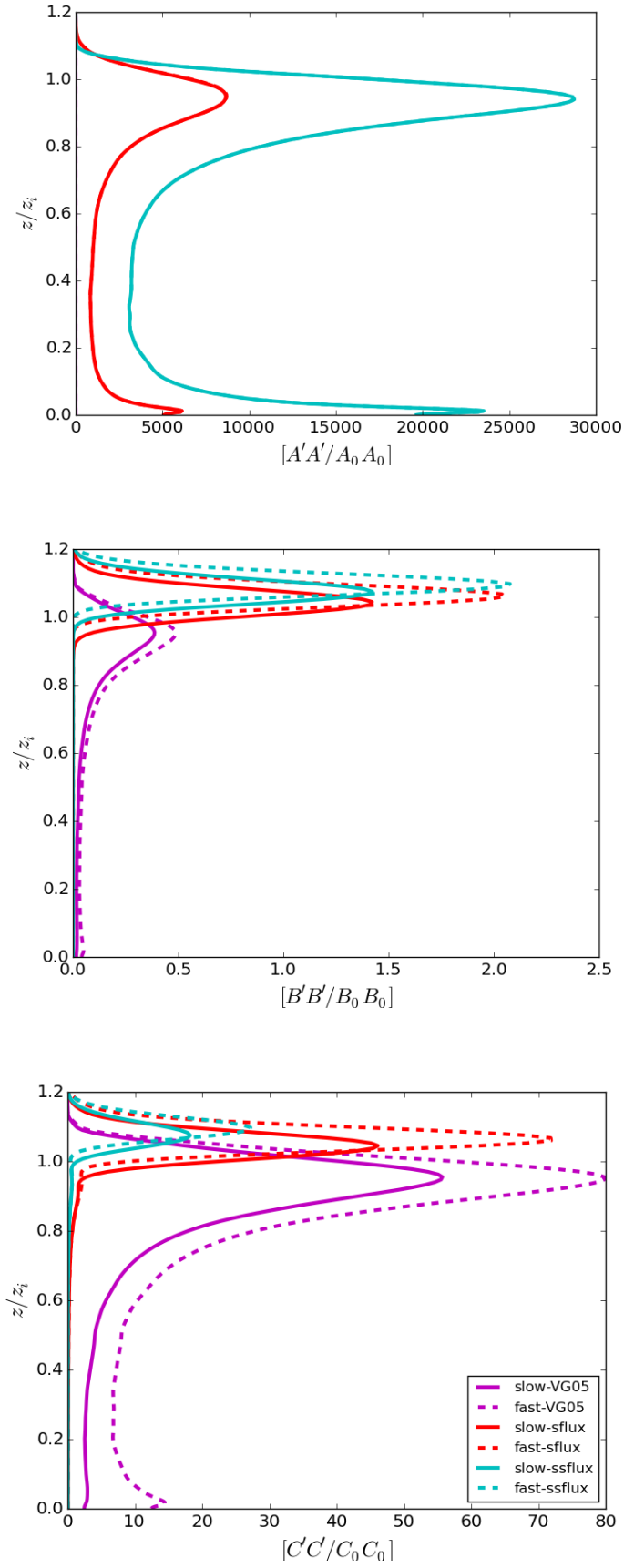


Figure 4: The vertical profiles of the concentration variances of Tracer A (*top panel*), B (*middle panel*) and C (*bottom panel*) normalised by the corresponding characteristic concentrations.

## (a) Homogeneous emissions

Case	$Da_{k A,i}$	$Da_{k B,i}$	$Da_{k A,f}$	$Da_{k B,f}$	$k_{eff}/k$
slow-VV05	7.25E-03	4.73E-04	8.44E-03	5.65E-04	0.9652
fast-VV05	7.25E-02	4.73E-03	7.97E-02	9.60E-04	0.8687
slow-mflux	7.72E-03	1.47E-03	1.99E-04	1.78E-01	0.235
fast-mflux	7.72E-02	1.47E-02	6.58E-04	1.78E+00	0.0455
slow-sflux	7.72E-03	1.08E-03	3.93E-05	4.16E-01	0.1225
fast-sflux	7.72E-02	1.08E-02	4.65E-05	4.16E+00	0.0304
slow-ssflux	7.72E-03	2.82E-03	3.08E-06	1.39E+00	0.0819
fast-ssflux	7.72E-02	2.82E-02	6.70E-07	1.39E+01	0.0226

## (b) Heterogeneous emissions

Case	$Da_{k A,i}$	$Da_{k B,i}$	$Da_{k A,f}$	$Da_{k B,f}$	$k_{eff}/k$
dx = 1 km					
slow-1km-VV05	1.46E-04	1.46E-04	1.42E-03	1.42E-03	1.0184
fast-1km-VV05	1.46E-03	1.46E-03	5.15E-03	5.15E-03	0.9094
slow-1km-sflux	3.53E-04	3.53E-04	1.41E-02	1.41E-02	0.5053
fast-1km-sflux	3.73E-03	3.73E-03	9.38E-02	9.41E-02	0.1365
dx = 2 km					
slow-2km-VV05	1.21E-04	1.21E-04	1.52E-03	1.53E-03	0.9952
fast-2km-VV05	1.22E-03	1.22E-03	5.95E-03	6.06E-03	0.7634
slow-2km-sflux	3.48E-04	3.48E-04	2.10E-02	2.13E-02	0.3068
fast-2km-sflux	3.46E-03	3.46E-03	1.70E-01	1.73E-01	0.0487
dx = 6 km					
slow-6km-VV05	1.82E-04	1.82E-04	2.12E-03	2.14E-03	0.665
fast-6km-VV05	1.80E-03	1.80E-03	1.37E-02	1.39E-02	0.2068
slow-6km-sflux	5.55E-04	5.55E-04	7.40E-02	7.52E-02	0.0312
fast-6km-sflux	5.40E-03	5.40E-03	7.13E-01	7.26E-01	0.0034

Table 1: The initial Kolmogorov Damköhler numbers  $Da_{k A,i}$  and  $Da_{k B,i}$ , and final Kolmogorov Damköhler numbers  $Da_{k A,f}$  and  $Da_{k B,f}$  with the resultant normalised effective chemical reaction rate  $k_{eff}/k$  in the DNS simulations with (a) homogeneous emissions and (b) heterogeneous emissions. Please refer to Table 2 of the manuscript for the corresponding Damköhler numbers.